JOURNAL OF MARITIME RESEARCH

Vol XXI. No. III (2024) pp 84–90

ISSN: 1697-4840, www.jmr.unican.es

A Comparative Study on Hydrodynamic Responses of Floating Offshore Wind Turbine Platforms in Regular Waves

Mir Tareque Ali[1], Md. Shariar Badon[1,*]

ARTICLE INFO

Article history:
Received 20 Feb 2024;
in revised from 17 Mar 2024;
accepted 13 May 2024.

Keywords:
Floating offshore wind turbine, Hydrostar, 3-D source distribution, Diffraction and radiation, Motion responses.

ABSTRACT

Floating Offshore Wind Turbine (FOWT) platforms have gained importance due to their adaptability to complex marine conditions in deep-sea environments. The objective of this paper is to perform hydrodynamic analysis of semisubmersible FOWT platforms in regular waves. A commercial hydrodynamic software named Hydrostar (introduced by Bureau Veritas) is adopted for numerical simulations of the present problem. The numerical simulations are based on linear three-dimensional (3-D) potential flow theory and the added mass and damping coefficients, first-order wave excitation forces and motion responses of FOWT platforms in six degrees of freedom are calculated. The frequency domain results are presented against wave circular frequency for different wave heading angles. The semisubmersible FOWT platform model used in this study features a central column and three offset columns having circular cross-sections with base at the bottom. Three different base geometries, namely circular, square, and hexagonal shape, are considered to understand their influence on the platform's hydrodynamic response. The numerical results are validated by comparing them with the published research. While the wave excitation forces and motion responses are influenced by wave heading angles, an in-depth comparative analysis of hydrodynamic results in the frequency domain for these three FOWT platform models indicates that variations in base geometry have negligible effects on the hydrodynamic behavior of these structures. The numerical results obtained from this research work may be helpful for hydrodynamic design of FOWT platforms.

1. Introduction.

Wind energy has been recognized as one of the key renewable energy sources, and its main development has been through the construction of onshore wind firms. However, due to the factors such as the lack of land space for the development of onshore wind firms, competing site usages, environmental impact etc., lead to the development of offshore wind energy in recent years. Moreover, offshore wind turbines tend to obtain better wind quality than do onshore wind turbines.

Thus, offshore wind turbines are expected to realize high generation efficiency. Most offshore wind turbines are installed in shallow water with bottom-fixed substructures in water depths of up to 50 m. Thus, in the future, offshore wind turbines are expected to be moved to deep water sites for these reasons, as well as for the stable and strong wind flow. For greater water depths, the FOWTs are unique solution to harness the offshore wind energy. The floating platforms of FOWT can be classified into three primary categories: a semisubmersible, a Spar buoy and a Tension Leg Platform (TLP). Compared to spar buoys and TLPs, the Semisubmersible platforms are more feasible in a variety of water depths and has lower costs of installation. The semisubmersible platforms have better hydrodynamic behavior due to the deep draft and they also use conventional mooring system.

Significant research on FOWT platforms began in the 1990s, with the first prototype built in 2007, sparking rapid expansion in research, development, and a multitude of platform designs

[1]Department of Naval Architecture and Marine Engineering, Bangladesh University of Engineering and Technology, Dhaka-1000.
[*]Corresponding author: Md. Shariar Badon . E-mail Address: 1812005@name.buet.ac.bd.

[1]. Meng, et al. [2] proposed analytical solutions to quantify the aerodynamic damping and hydrodynamic damping for the FOWT platform and the analytical expressions of damping and simplified model was successfully verified against softwares like FAST and Aqwa. Kim, et al. [3] performed time domain simulation to investigate the characteristics of wave-induced motion of a TLP-type combined wind-wave energy platform to reduce the variability of energy extraction. Zhou, et al. [4] studied the effect of focused wave on floating offshore wind turbine platform by conducting a comparative study of CFD simulation and model test. An experimental study for motion response analysis was performed by Amin et al. [5] to investigate the feasibility of integrating a wind turbine into the same floating desalination plants platform. Ahn, et al. [6] performed a model test of a 10 MW floating offshore wind turbine, and then the model test results were verified by comparing them to the numerical results. Chu, et al. [7] used a frequency domain approach for analyzing wind and wave coupling effect on motion responses of an integrated offshore fish cage and wind turbine. Wang, et al. [8] investigated the effect of damping induced by wind, current and mooring system on the floating foundation response on floating wind turbine.

In the present study, a commercial hydrodynamic software named Hydrostar was used for numerical simulations to perform the hydrodynamic analysis of semisubmersible FOWT platforms in regular waves. The added mass and damping coefficients, first-order wave excitation forces and motion responses of FOWT platforms in six degrees of freedom are calculated and presented against wave circular frequency for different wave heading angles. The FOWT platform model used in this study features a central column and three offset columns having circular cross-sections with base at the bottom. Three different base geometries, namely circular, square, and hexagonal, are considered for the present investigation. The numerical results for circular base are validated by comparing them with the published research. Through a comparative analysis of these three FOWT platform models, the findings suggested that changes in base geometry do not significantly impact the hydrodynamic behavior of these structures.

2. Mathematical Formulation.

Consider, a 3-D body of arbitrary shape is freely floating in water with regular waves and the fluid is assumed to be incompressible, inviscid, and irrotational. The amplitudes of the motions of the oscillating body in the water of uniform depth by a long-crested regular wave are assumed to be small. A Cartesian coordinate system O-XYZ is defined, with OXY plane being the undisturbed mean free water surface and Z axis pointing vertically upwards. When the floating body is at its equilibrium position, the Z axis passes through the center of mass of the body as shown in Fig. 1. In regular waves a linear potential Φ, which is a function of space and of time, can be written as a product of space-dependent term and a harmonic time-dependent term as follows:

$$\Phi(x, y, z; t) = Re\left[\phi(x, y, z).e^{-i\omega t}\right] \tag{1}$$

where $\phi(x, y, z)$ is time independent quantity and the potential function $\phi(x, y, z)$ can be separated into contributions from all modes of motion of the bodies and from the incident and diffracted wave fields as follows:

$$\phi = -i\omega[(\phi_0 + \phi_7)\zeta_a + \sum_{j=1}^{6}\left(X_j\phi_j\right)] \tag{2}$$

where ϕ_0 is the incident wave potential, ϕ_7 is the diffraction wave potential, ϕ_j represents potential due to motion of body in the jth mode i.e., radiation wave potential, X_j stands for the motion of body in jth mode and ζ_a is the incident wave amplitude. The incident wave potential can be expressed as:

$$\phi_0 = \frac{g}{\omega^2}\frac{\cosh[k(z+h)]}{\cosh kh}e^{ik(xcos\beta+ysin\beta)} \tag{3}$$

where β is the angle of incident wave relative to the positive x-axis, h is the depth of water, g is the gravitational acceleration and k is the wave number. The individual potentials are the solutions of Laplace equation and they need to satisfy linearized free surface condition, boundary condition on the sea floor and on the wetted surface of the floating bodies and the boundary condition at infinity i.e., the radiation condition. According to the 3-D source distribution method, the potentials ϕ_7 and ϕ_j can be expressed in terms of well-known Green functions and as a result, boundary conditions are reduced to only on the wetted surfaces of the bodies [10].

Having the velocity potentials, the pressure at any point on the structure can be determined from linearized Bernoulli's equation:

$$p = -\rho\frac{\partial\Phi}{\partial t} = i\rho\omega\,\phi\,e^{-i\omega t} \tag{4}$$

Substituting Equation (2) into the Equation (4) we can write,

$$p = \rho\omega^2[(\phi_0 + \phi_7)\zeta_a + \sum_{j=1}^{6}\left(X_j\phi_j\right)]\,e^{-i\omega t} \tag{5}$$

Consequently, the wave exciting forces (F_k), the added mass coefficients (a_{kj}), and damping coefficients (b_{kj}), can be written respectively as follows:

$$F_k = -\rho\omega^2\zeta_a e^{-i\omega t}\int(\phi_0 + \phi_7).n_k.ds \tag{6}$$

where k = 1,2, ….6

$$a_{kj} = -Re\left[\rho\iint_s \phi_j.n_k.ds\right] \tag{7}$$

where k = 1,2, ….6

$$b_{kj} = -Im\left[\rho\omega\iint_s \phi_j.n_k.ds\right] \tag{8}$$

where k = 1,2, ….6

Upon solving the exciting forces, added mass coefficients, damping coefficients, the equations of six rigid body motions in the frequency domain can be written as: X_j

$$sum_{j=1}^{6}\left(m_{kj} + a_{kj}\right)\ddot{X}_j + b_{kj}\dot{X}_j + c_{kj}X_j = F_k \tag{9}$$

where k = 1,2, ….6

where m_{kj}, a_{kj}, b_{kj}, c_{kj} are the body inertia matrix, added mass coefficient matrix, damping matrix and hydrodynamic restoring matrix respectively in k^{th} mode due to motion in j^{th} mode, X_j is the vector containing translational and rotational oscillations about the co-ordinate axes and F_k is the wave exciting force matrix.

Figure 1: Top and front view of the FOWT platform with circular base showing wave heading angles.

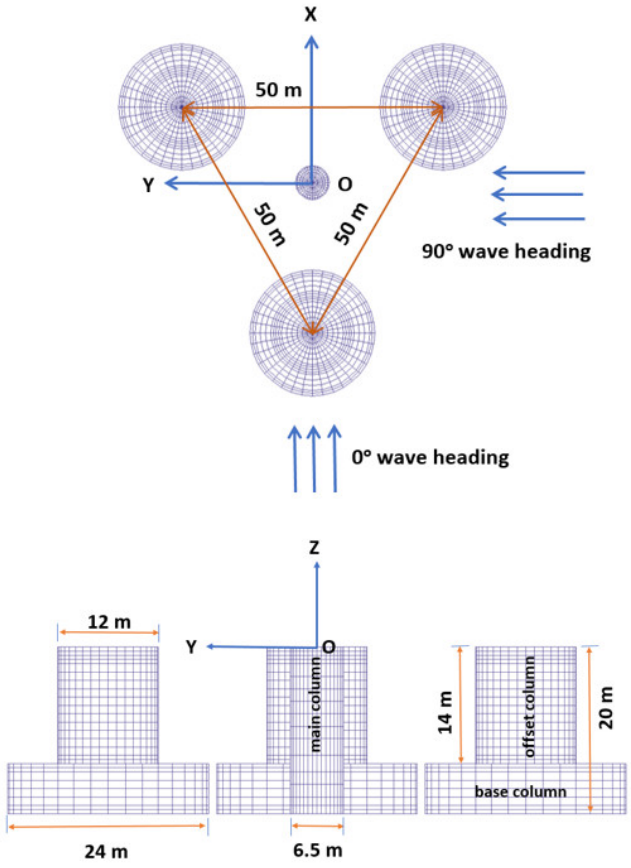

Source: Authors.

3. Results and Discussions

The OC4 DeepCwind semisubmersible [10] was selected as the model for the Floating Offshore Wind Turbine (FOWT) platform in this study. This platform comprises a primary column connected to the wind turbine tower and three offset columns. To simplify the model, the smaller diameter connecting elements between these columns are omitted, as illustrated in Fig. 1. The main column has a diameter of 6.5 meters, while the offset and base columns measure 12 meters and 24 meters in diameter, respectively. The three offset columns are arranged in an equilateral triangle formation with sides measuring 50 meters in length, and the center of the main column aligns with the centroid of this triangle. In this paper, we explore three different base column geometries: circular, square, and hexagonal, as depicted in Fig. 2. These geometries are considered by varying the cross-sectional area of the base column. The vertical height of the base columns is fixed at 6 meters, and the semisubmersibles have a draft of 20 meters, with a water depth of 200 meters used for the analysis. The total mass of the FOWT platform is 1.3473E+7 kilograms, and its center of mass is located 13.46 meters below the still water level (SWL). To conduct numerical simulations for this study, we employed a commercial hydrodynamic software known as Hydrostar, which is based on linear 3-D potential flow theory. Fig. 2 displays a 3-D mesh arrangement view of the FOWT platforms with different base geometries. Three catenary mooring lines with equivalent mooring line stiffness of 7.536E+8 N, spreading symmetrically about the platform Z-axis is deployed to secure the platform [10].

Figure 2: 3-D mesh arrangement view of the FOWT platforms with different base geometry.

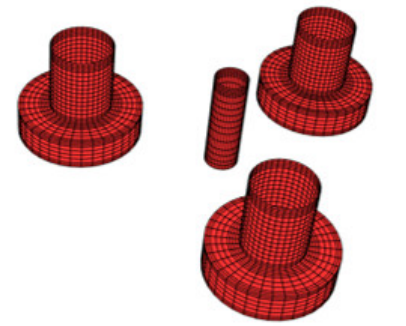

(a) circle (5760 panels)

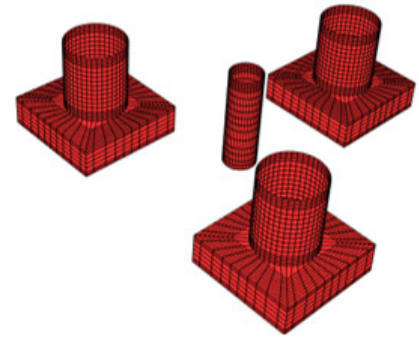

(b) square (6558 panels)

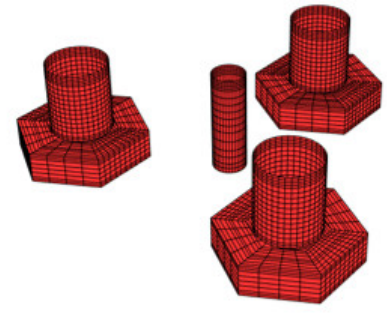

(c) hexagon (5760 panels)

Source: Authors.

The figure in Fig. 3 displays the added mass coefficients for surge, heave, and yaw modes for the three models, as well as the published results by Robertson et al. [10] for the circle model. It is evident from these figures that there is a satisfactory agreement between the current study's results and the published data. Furthermore, the added mass coefficients for all three models exhibit a remarkable similarity. Notably, Fig. 3(a) shows that for lower frequencies (<0.2 Hz), the surge added mass coefficient is more pronounced, with a prominent peak at 0.15 Hz, followed by a sharp decline that maintains a consistent magnitude for higher frequencies (>0.2 Hz). The heave added mass coefficients for the three models exhibit minimal variation with wave frequencies as shown in Fig. 3(b). This consistency can be attributed to the fact that the effect of added mass for heave predominantly influences the bottom of the vertical cylinder, which is relatively distant from the free water surface. In Fig. 3(c), it is again observed that for lower frequencies (<0.2 Hz), the yaw added mass coefficient is larger, with a peak at 0.15 Hz, followed by a sharp decline maintaining a constant magnitude for higher frequencies (>0.2 Hz).

Figs. 3(d), 3(e) and 3(f) present the radiation damping coefficients for surge, heave, and yaw modes for the three models, alongside the published results by Robertson et al. [10] for the circle model. Similar to the added mass coefficient findings, there is a high degree of agreement between the current and published results for damping coefficients. The surge radiation damping coefficients for all three bottoms shows excellent similarity, with the highest peak occurring around 0.2 Hz. After that there is a slight fall and then a smaller peak occurs around 0.25 Hz shown in Fig. 3(d). Similarly, the damping coefficients for all three models exhibit a consistent pattern for heave with the highest peak occurring around 0.2 Hz. In Fig. 3(e), at a frequency of 0.2 Hz, there is a slight deviation in the heave radiation damping for the square model compared to the other two models. For the pitch mode, the damping coefficients are very similar to each other and have excellent consistency with the published results by Robertson et al. [10]. The highest peak in this case also occurs near 0.2 Hz frequency and after that there is a sharp decline which continues to 0.4 Hz. For the rest of the graph, it maintains a consistent magnitude.

Fig. 4(a) illustrates the first-order surge wave excitation forces for the three models at wave headings of 0°, 45°, and 90°. As expected, the surge forces for a 0° wave heading are greater than for a 45° heading, as the surge mode aligns with the wave direction. Two peaks are discernible at frequencies around 0.1 Hz and 0.2 Hz.

Conversely, due to the asymmetry of the water-plane area for a 90° wave heading, a very small magnitude of surge excitation force is observed. The first-order heave wave excitation forces are also depicted in Fig. 4(b) for wave headings of 0°, 45°, and 90°. For the most part, the three models produce similar results for all three wave headings, except within the frequency range of 0.1 Hz to 0.2 Hz, where the exciting forces gradually decrease for 0°, 45°, and 90° wave headings, respectively. Furthermore, Fig. 4(c) displays the first-order pitch wave exciting forces at wave headings of 0°, 45°, and 90°. Once again, the three models yield consistent results for each wave heading angle. Interestingly, the exciting forces for a 0° wave heading are greater than for the other two headings. This unexpected result may be attributed to the structural asymmetry at a 90° wave heading.

Fig. 5(a) provides insight into the surge motion response of the three models for wave headings of 0°, 45°, and 90°. Consistently, the three models exhibit similar responses for each wave heading. Surge motion predominates at lower frequencies (<0.2 Hz), with greater motion observed for a 0° wave heading. Conversely, since the surge mode is orthogonal to the 90° wave heading, surge motion is nearly negligible at this orientation. Fig. 5(b) also presents the heave motion response of the three models for wave headings of 0°, 45°, and 90°.

Once more, the three models demonstrate analogous results for each wave heading angle. Notably, the absence of viscous damping in the linear potential theory leads to excessive heave motion, particularly near the heave resonance frequency of 0.5 Hz. Lastly, Fig. 5(c) illustrates the pitch motion response of the three models for wave headings of 0°, 45°, and 90°. Similarly, the three models exhibit consistent responses for each wave heading angle. Pitch motion is most pronounced at lower frequencies (<0.2 Hz), with greater motion observed for a 0° heading, gradually decreasing for 45° and 90° wave headings, respectively. The pitch motion results reveal a prominent peak in proximity to the heave resonance frequency of 0.5 Hz.

Conclusions.

The frequency domain hydrodynamic analysis is performed for semisubmersible FOWT platforms in regular waves using a commercial hydrodynamic software named Hydrostar. Three different base geometries, namely circular, square, and hexagonal, are considered for the present investigation.

Surge and yaw added mass coefficients are more pronounced for lower frequencies (<0.2 Hz), with a prominent peak at 0.15 Hz, followed by a sharp decline that maintains a consistent magnitude for higher frequencies (>0.2 Hz). The heave added mass coefficients for the three models exhibit minimal variation with wave frequencies.

The surge, heave and yaw damping coefficients for all the three models exhibit a consistent pattern, with the highest peak occurring around 0.2 Hz. In general, surge, heave and pitch the first-order wave excitation forces and motion responses gradually decreases for 0°, 45°, and 90° wave headings. The absence of viscous damping in the linear potential theory leads to excessive heave and pitch motions, particularly near the heave and pitch resonance frequencies close to 0.5 Hz. The frequency domain simulations for three FOWT platform models indicate that variations in base geometry have negligible effects on the hydrodynamic behavior of these structures.

Figure 3: Added mass and damping coefficients for surge(11), heave(33) and yaw(66) mode of the FOWT platforms.

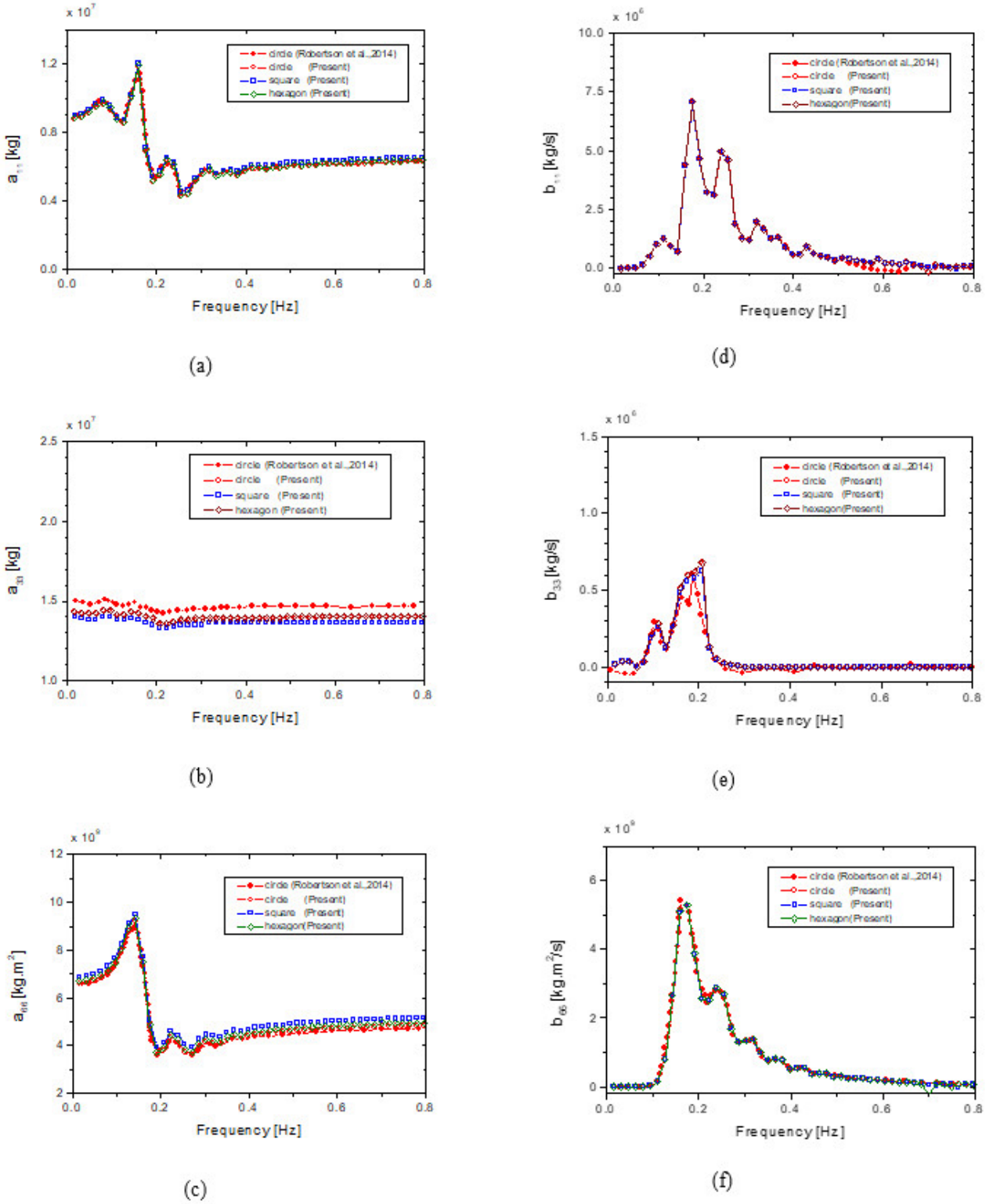

Source: Authors.

Figure 4: Surge(F_1), heave(F_3) and pitch(F_5) wave- excitation forces for the FOWT platforms.

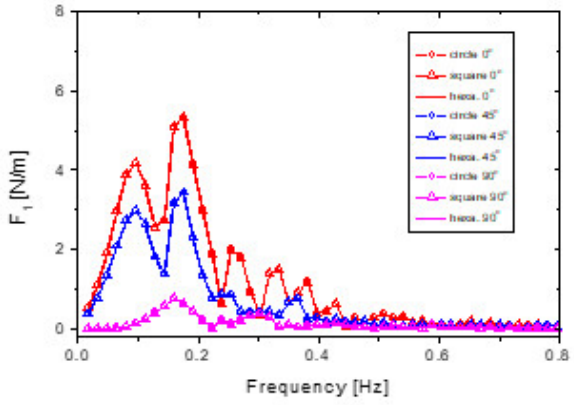

(a)

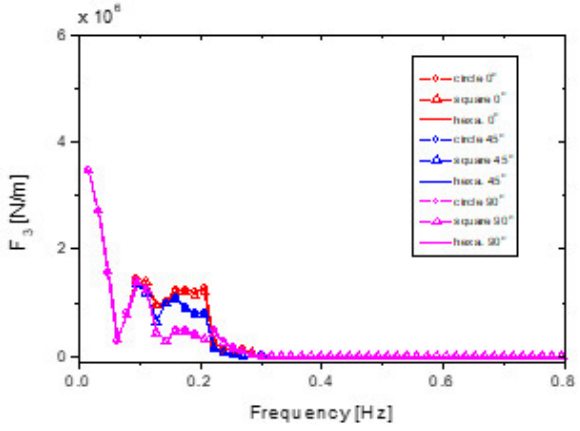

(b)

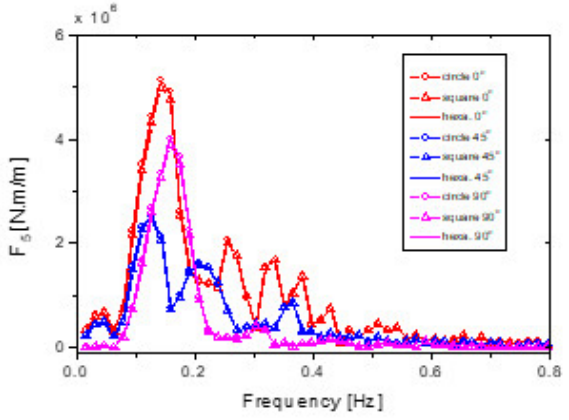

(c)

Source: Authors.

Figure 5: Surge(X_1), heave(X_3) and pitch(X_5) motion responses for the FOWT platforms.

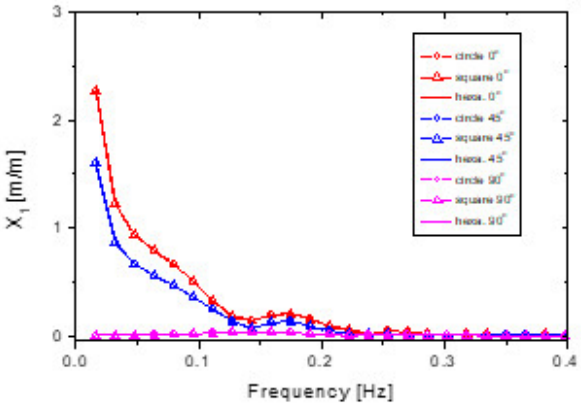

(a)

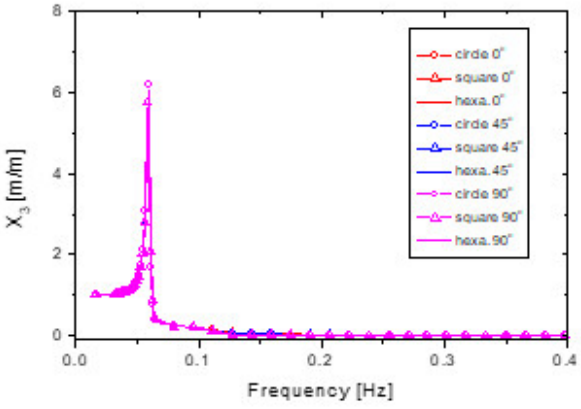

(b)

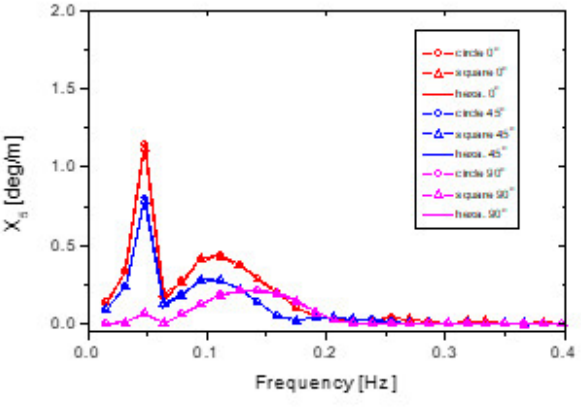

(c)

Source: Authors.

References.

1. E. C. Edwards, A. Holcombe, S. Brown, E. Ransley, M. Hann, D. Greaves "Evolution of Floating Offshore Wind Platforms: A Review of at-Sea Devices", (Renewable and Sustainable Energy Reviews, 183, 2023).
2. Q. Meng, X. Hua, C. Chen, S. Zhou, F. Liu, Z. Chen "Analytical study on the aerodynamic and hydrodynamic damping of the platform in an operating spar-type floating offshore wind turbine", (Renewable Energy, 198,2022) pp. 772-788
3. H. Kim, E. Min, S. Heo, W. C. Koo "Motion Analysis of a Wind-Wave Energy TLP Platform Considering Second-order Wave Forces", (Journal of Ocean Engineering Technology, 36(6), 2022) pp. 390-402.
4. Y. Zhou, Y. Cai, H. Zhao, W. Shi, X. Li, X. Zeng "Comparative Study of Hydrodynamic Responses of Floating Offshore Wind Turbine Platform Under Focused Wave Using Experiment and OpenFOAM", Proceedings of the 33rd International Ocean and Polar Engineering Conference,2023) pp. ISOPE-I-23-069.
5. I. Amin, S. Dai, S. Day, M. Ali, A. Balah, H. Shawky, S. Oterkus, E. Oterkus, "Experimental study on the motion response of an integrated floating desalination plant and offshore wind turbine on a non-ship platform", (Ocean Engineering, 234, 2021) pp. 109275
6. H. Ahn, H. Shin "Experimental and Numerical Analysis of a 10 MW Floating Offshore Wind Turbine in Regular Waves", (Energies, 13, 2020) pp. 2608
7. Y. I. Chu, C. M. Wang, H. Zhang "A Frequency Domain Approach for Analyzing Motion Responses of Integrated Offshore Fish Cage and Wind Turbine Under Wind and Wave Actions", (Aquacultural Engineering, 97, 2022) pp. 102241.
8. K. Wang, C. Ji, H. Xue, W. Tang "Frequency Domain Approach for the Coupled Analysis of Floating Wind Turbine System", (Ships and Offshore Structures, 12(6), 2017) pp. 767-774.
9. M. A. Amif, P. Biswas, S. A. Sakib, M. T. Ali "Hydrodynamic Analysis of a Semisubmersible Type Offshore Structure in Regular Waves", (Proceeding of MARTEC 2020).
10. A. Robertson, J. Jonkman, M. Masciola, H. Song, A. Goupee, A. Coulling, C. Luan "Definition of the Semisubmersible Floating System for Phase II of OC4", (National Renewable Energy Laboratory, NREL/TP-5000-60601, 2014).